Molecular Physics
Vol. 110, Nos. 15–16, 10–20 August 2012, 1681–1691

INVITED ARTICLE

On the use of quadratic approximants to model diatomic potential energy curves†

David Z. Goodson*

Department of Chemistry & Biochemistry, University of Massachusetts Dartmouth, North Dartmouth, Massachusetts, USA

(*Received 11 December 2011; final version received 22 February 2012*)

Quadratic approximants are shown to have an appropriate functional form for modelling the mathematical structure of the full configuration interaction energy as a function of internuclear distance. The problem of spurious singularities is discussed. Quadratic approximants with additional constraints are constructed so as to avoid spurious singularities and to have the correct dissociation limits. It is shown that these approximants are appropriate for interpolating between computed *ab initio* energies. The method is tested with a set of full configuration interaction energies for the hydrogen fluoride molecule. The approximants are shown to give an accurate interpolation through the region of moderate bond stretching where direct approximate *ab initio* computations are difficult. A procedure for parameterizing the approximants to empirical data is developed.

Keywords: molecular potential energy functions; quadratic approximants; full configuration interaction; avoided crossings; singularity analysis

1. Introduction

The molecular potential energy hypersurface provides a bridge from fundamental physical theory to chemical applications. Within the Born–Oppenheimer approximation, an electronic Schrödinger equation is formulated for fixed nuclear configurations. The electronic energy is then added to the potential energy of nucleus–nucleus repulsion. The result is a continuous function, $E(\boldsymbol{x}_1, \boldsymbol{x}_2, \boldsymbol{x}_3, \ldots)$ of coordinates $\boldsymbol{x}_i$ specifying the relative positions of the nuclei, that can be used as a potential energy function for the nuclear dynamics.

There are three commonly used approaches for obtaining this function. (1) A series approximation is generated about a stable minimum of the potential energy [1,2]. (2) An arbitrary functional form is parameterized to provide a global model of the potential [3–8]. (3) A numerical interpolation is developed to reproduce a set of discrete points and smoothly connect between them [9–11]. These approaches can be very useful for practical applications but they make no serious attempt to analytically model the functional form of the actual function E.

A systematic procedure for constructing a diatomic potential energy curve by modelling its fundamental mathematical structure was proposed by Jordan [12,13]. He used a quadratic approximant to model the branch-point singularities of E in the plane of the internuclear distance treated as a variable over the complex numbers. The branch points correspond to avoided crossings between the ground state and an excited state of the same symmetry. The quadratic approximant has two branches. One branch interpolates between known ground state energy values while the other branch models an excited state.

Here Jordan's method is extended by imposing constraints at known limits, in order to construct an analytic functional form for the global potential energy function. Linear algebraic equations are formulated for the parameterization and then possible applications are illustrated using a data set of full configuration interaction (FCI) energies for the hydrogen fluoride molecule.

2. Theory

2.1. *Mathematical structure of the energy function*

Consider the electronic Schrödinger equation for a diatomic molecule,

$$\hat{H}(x)\Psi = E\Psi. \tag{1}$$

The Hamiltonian operator $\hat{H}$ depends parametrically on the internuclear distance x. Let us express the eigenfunctions as linear combinations of n

---

*Email: dgoodson@umassd.edu

†This paper is dedicated with affection to my mentor Dudley Herschbach.

ISSN 0026–8976 print/ISSN 1362–3028 online

http://dx.doi.org/10.1080/00268976.2012.670282
http://www.tandfonline.com

orthonormal functions f_i from the Hilbert space. These functions are a basis for a finite-dimension subset of the Hilbert space. By diagonalizing the Hamiltonian matrix $\mathbf{H}(x)$ comprised of the elements $H_{i,j}(x) = \langle f_i|\hat{H}(x)|f_j\rangle$, one can obtain variational upper bounds to the energy eigenvalues $\tilde{E}_k$, which approach the true eigenvalues E_k in the limit $n \to \infty$.

The configuration interaction method uses spin-adapted Hartree–Fock wavefunctions expressed as linear combinations of the n-dimensional basis set. These wavefunctions are then used to compute the Hamiltonian matrix [14]. If the determinants corresponding to all possible excitations are included, then we have the *full* configuration interaction method. The computational cost scales as $n!$, which makes this too expensive for general use, but with current computational resources it is quite feasible for benchmark computations for molecules in which the number of correlated electrons is on the order of 10.

The $H_{ij}(x)$ are *entire* functions of x, which is to say that they are nonsingular (i.e. finite, single-valued, with a well-defined derivative) at all finite points in the plane of complex x. The resulting eigenfunctions $\tilde{E}_k(x)$ are not entire, but have a rich structure of branch-point singularities, as described by the following theorem [15–19]:

Theorem 2.1: *Consider an* $n \times n$ *matrix eigenvalue problem* $\mathbf{H}(x)\mathbf{v} = \tilde{E}\mathbf{v}$ *in which* $\mathbf{H}$ *is an Hermitian matrix and the elements of* $\mathbf{H}$ *are entire functions of* x. *Assume that no two eigenvalues are equal at any real value of* x. *Let* $\tilde{E}_0(x), \tilde{E}_1(x), \tilde{E}_2(x), \ldots, \tilde{E}_n(x)$ *be the eigenvalues of a given symmetry (e.g. with the same angular momentum quantum numbers) in order of increasing value. Then for each pair* $\tilde{E}_k(x)$, $\tilde{E}_\ell(x)$ *there exists a complex-conjugate pair of branch points* $x_{k\ell}$, $x^*_{k\ell}$, *with non-zero imaginary parts, that connect the functions* $\tilde{E}_k(x)$ *and* $\tilde{E}_\ell(x)$. *In the neighbourhood of* $x_{k\ell}$ *the functions behave as*

$$\tilde{E}_{k\ell} \pm \gamma_{k\ell}(x - x_{k\ell})^{1/2},$$

with constants $\gamma_{k\ell}$ *and with* $\tilde{E}_k(x_{k\ell}) = \tilde{E}_\ell(x_{k\ell}) = \tilde{E}_{k\ell}$.

Thus, each branch $\tilde{E}_k(x)$ of the FCI energy function will have $n-1$ complex-conjugate pairs of square-root branch points somewhere in the complex plane off the real axis. If one plots the eigenvalues over a domain of real x they exhibit avoided crossings, avoided because there are no branch points on the real axis. The real part of the branch point location is about equal to the real x value at the closest approach between the corresponding pairs of eigenstates. The imaginary part is approximately proportional to the energy difference at the closest approach and to the amount of overlap of the wavefunctions.

2.2. *Quadratic approximants*

Jordan's method consists of constructing a double-valued approximant $S(x)$, for the lowest two eigenvalues, such that S contains square-root branch points. The approximant is constructed from three polynomials,

$$P(x) = p_0 + p_1 x + p_2 x^2 + \cdots p_L x^L, \tag{2}$$

$$Q(x) = 1 + q_1 x + q_2 x^2 + \cdots q_M x^M, \tag{3}$$

$$R(x) = r_0 + r_1 x + r_2 x^2 + \cdots r_N x^N, \tag{4}$$

such that

$$Q(x_k)\tilde{E}_k^2 - P(x_k)\tilde{E}_k + R(x_k) = 0 \tag{5}$$

for each point from a data set

$$\{(x_1, \tilde{E}_1), (x_2, \tilde{E}_2), (x_3, \tilde{E}_3), \ldots (x_K, \tilde{E}_K)\}.$$

This gives a set of K linear algebraic equations that uniquely determines the values of the polynomial coefficients p_i, q_i, and r_i. For a set of K data points, the polynomial degrees satisfy the constraint

$$L + M + N + 2 = K. \tag{6}$$

The approximant is obtained from Equation (5) using the quadratic formula,

$$S(x) = \frac{1}{2Q}\left(P \pm \left(P^2 - 4QR\right)^{1/2}\right). \tag{7}$$

We will label S according to the degrees of P, Q, and R, with an index $[L/M, N]$. Each choice of the index yields a different approximant to the same data set. Square-root branch points occur at roots of the discriminant polynomial

$$D(x) = P^2 - 4QR. \tag{8}$$

Equation (7) is called a *quadratic approximant* (QA). These approximants were originally proposed in the 1890s by Padé [20] as a method for summing Taylor series. (Instead of parameterizing to a set of points, the polynomial coefficients are determined from the condition that the Taylor series of one of the roots of S agree with the Taylor series of interest at each power of the expansion variable up to some specified series order.) They were largely unexploited until being rediscovered by mathematicians in the 1970s. Jordan seems to have been the first to apply them to a problem in chemical physics. Since then, they have found many applications to perturbation theories for atomic and molecular problems [21].

Figure 1 compares interpolation using a QA with interpolation using a polynomial, for a set of FCI

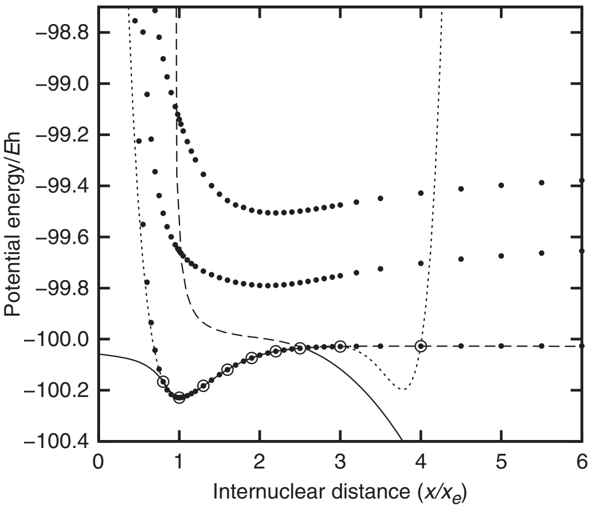

Figure 1. Potential energies for the ground state and the first two excited states with the same symmetry as the ground state for the hydrogen fluoride molecule. The solid points are FCI energies. The dotted curve shows the eighth-degree polynomial that interpolates between the nine circled points. The solid and dashed curves show the two solutions for the [1/3, 3] quadratic approximant.

energies for the hydrogen fluoride molecule. (These FCI energies will be presented and discussed in Section 3.) The dotted curve is a polynomial interpolation between the nine circled points. It does a poor job of extrapolating beyond the region covered by the data set. At large x it becomes infinite, where it ought to approach a constant value. At small x it approaches a constant, where it ought to become infinite.

The solid curves show the two roots of $S_{[1/3,3]}(x)$, the QA with index [1/3,3]. The choice of index is important. In the limit of large x, Equation (7) becomes

$$S(x) \sim \frac{1}{2q_M x^M}\left(p_L x^L \pm \left(p_L x^{2L} - 4q_M r_N x^{M+N}\right)^{1/2}\right). \tag{9}$$

This will approach a non-zero constant only under the following conditions:

$$L = M,\ N \leq M \quad \text{or} \quad N = M,\ L \leq M. \tag{10}$$

With $K = 9$ as the number of data points, the only acceptable approximant indices are [3/3, 1] and [1/3, 3], which give essentially identical results. One of the roots of the approximant does behave qualitatively correctly at large x. However, the small-x behaviour is wrong, and the 'excited' state seems to cross the 'ground' state, falling below it at large x.

Although the performance of the QA here is admittedly not very good, it is not without promise. The branch points of $S(x)$ are found at the roots of the discriminant polynomial $P^2 - 4QR$, which in this case are

$$2.1297 \pm 0.8100\mathrm{i},\quad 2.2388 \pm 0.0032\mathrm{i},\quad 0.8402 \pm 0.1420\mathrm{i},$$

with x in units of the equilibrium bond distance x_e. The first branch-point pair is in fact quite accurate. The closest approach in this case occurs at $x = 2.37x_e$, which could be modelled rather well by the branch point at 2.1297± 0.8100i if it were not for the presence of the spurious pair of branch points at $2.2388 \pm 0.0032\mathrm{i}$. Nearly coincident spurious branch points are a common phenomenon with QAs. In this case they introduce a factor of $(x - 2.2388 - 0.0032\mathrm{i})(x - 2.2388 + 0.0032\mathrm{i})$ into the discriminant polynomial, which is very nearly equal to the perfect square $(x - 2.2388)^2$. The square root of a perfect square is nonsingular. This branch point pair does not correspond to a branch point pair of the true energy function, but it has a significant effect on the behaviour of the approximant, causing an extremely sharp avoided crossing. (Contrary to appearances, the two curves do not actually cross.)

2.3. *Constrained approximants*

Our strategy is to improve the accuracy of the QA by constraining it to have the desired behaviour in known limits. We begin with an analysis of the $x \to \infty$ limit. The desired behaviour is

$$\lim_{x\to\infty} S(x) = \begin{cases} \tilde{E}_{\mathrm{d},1}, \\ \tilde{E}_{\mathrm{d},0}, \end{cases} \tag{11}$$

where $\tilde{E}_{\mathrm{d},0}$ and $\tilde{E}_{\mathrm{d},1}$ are the energies of the dissociated fragments for the ground state and the first excited state, respectively. For large x, Equation (5) becomes

$$x^M q_M \tilde{E}_\mathrm{d}^2 - x^L p_L \tilde{E}_\mathrm{d} + x^N r_N \sim 0, \tag{12}$$

where $\tilde{E}_\mathrm{d}$ is $\tilde{E}_{\mathrm{d},0}$ or $\tilde{E}_{\mathrm{d},1}$. Suppose that $M = N$ and $L < M$. Then the middle term disappears for $x \to \infty$ and we obtain the two solutions $\tilde{E}_\mathrm{d} = \pm(-r_M/q_M)^{1/2}$. Either both solutions are pure imaginary or one is negative real while the other is positive real. We want $\tilde{E}_{\mathrm{d},0}$ and $\tilde{E}_{\mathrm{d},1}$ to be real numbers with the same sign. Consider the case $M = L$, $N < M$. Then we have only a single branch, with $\tilde{E}_\mathrm{d} = p_M/q_M$. It follows that the only reasonable choice is a diagonal index,

$$L = M = N. \tag{13}$$

This gives the constraint equations

$$q_M\tilde{E}_{\mathrm{d},0}^2 - p_M\tilde{E}_{\mathrm{d},0} + r_M = 0, \quad q_M\tilde{E}_{\mathrm{d},1}^2 - p_M\tilde{E}_{\mathrm{d},1} + r_M = 0, \tag{14}$$

which allow arbitrary values for $\tilde{E}_{\mathrm{d},0}$ and $\tilde{E}_{\mathrm{d},1}$. Combining these equations to eliminate p_M, we obtain

$$r_M = \tilde{E}_{\mathrm{d},0}\tilde{E}_{\mathrm{d},1}q_M. \tag{15}$$

Eliminating r_M, we obtain

$$p_M = (\tilde{E}_{\mathrm{d},0} + \tilde{E}_{\mathrm{d},1})q_M. \tag{16}$$

Consider the $x \to 0$ limit, the limit of united nuclei. The electronic energy remains finite but the internuclear potential introduces a first-order pole. Either we should apply the QA just to the electronic energy before adding the internuclear potential, using Equations (2)–(4), or we should design the QA so that

$$S(x) \sim Z_\mathrm{A}Z_\mathrm{B}/x \tag{17}$$

in the limit $x \to 0$ for both branches of the approximant. (We are using atomic units, with energy in hartrees and distance in bohrs. Z_A and Z_B are the atomic numbers of the two nuclei.) The function $\tilde{E}(x)$ can be expanded in a Laurent series,

$$\tilde{E}(x) \sim \epsilon_{-1}x^{-1} + \epsilon_0 + \epsilon_1 x + \epsilon_2 x^2 + \cdots + \epsilon_m x^m. \tag{18}$$

Substituting this into the quadratic equation gives the asymptotic equation

$$Q\tilde{E}^2 - P\tilde{E} + R \sim \mathcal{O}(x^{m+1}). \tag{19}$$

After collecting terms according to the power of x, it becomes clear that in order to implement Equation (17) our polynomials should have the forms

$$P(x) = p_{-1}x^{-1} + p_0 + p_1x + p_2x^2 + \cdots + p_Mx^M, \tag{20}$$

$$Q(x) = 1 + q_0 + q_1x + q_2x^2 + \cdots + q_Mx^M, \tag{21}$$

$$R(x) = r_{-2}x^{-2} + r_{-1}x^{-1} + r_0 + r_1x + r_2x^2 + \cdots + r_Mx^M. \tag{22}$$

The $x \to 0$ limit yields an expression for ϵ_{-1} in terms of p_{-1} and r_{-2},

$$\epsilon_{-1} = \frac{1}{2}\left(p_{-1} \pm \left(p_{-1}^2 - 4r_{-2}\right)^{1/2}\right). \tag{23}$$

We want both states to have the pole at $x = 0$ with the same residue ϵ_{-1}. This is accomplished with the constraints

$$p_{-1} = 2\epsilon_{-1}, \quad r_{-2} = \epsilon_{-1}^2, \tag{24}$$

with

$$\epsilon_{-1} = Z_\mathrm{A}Z_\mathrm{B}. \tag{25}$$

Looking at the explicit expression for $S(x)$, Equation (7), one can anticipate another kind of spurious singularity. Consider what happens when the value of the denominator polynomial, $Q(x)$, passes through zero. In the limit of small Q, we have

$$S(x) \sim P\,\frac{1 \pm (1 - 2QR/P^2)}{2Q}. \tag{26}$$

The '$-$' branch is nonsingular for $Q = 0$, with the finite value R/P. The '$+$' branch, however, has a first-order pole, becoming infinite as P/Q. This happens at each of the M roots of $Q(x)$. In the absence of any spurious branch points on or very close to the positive real axis, the '$-$' branch describes the ground state energy, and the accuracy of that branch of the approximant will not be significantly affected by this phenomenon. However, the description of the excited state will be qualitatively incorrect.

To prevent any positive real roots from appearing in Q, let us write

$$Q(x) = 1 + q_Mx^M \tag{27}$$

and then treat q_M as an *arbitrary* parameter. If q_M is set to a positive number, then the poles will be at

$$x = q_M^{-1/M}\exp[\mathrm{i}\pi(2m+1)/M], \quad m = 1, 2, \ldots, M, \tag{28}$$

and this can never lie on the positive real axis. It will be seen in Section 3.1 that there will be a range of q_M values for which the branch-point structure of the QA is reasonable and for which the result is insensitive to the choice of q_M. Thus, an added benefit of having q_M as a free parameter is the opportunity to choose its value so as to optimize the description of the branch-point structure. This will be used to advantage in Section 3.2.

We have imposed five constraints: Equations (15) and (16) for the large-x behaviour, which determine r_M and q_M; Equations (24) for the small-x behaviour, which determine p_{-1} and r_{-2}; and the treatment of q_M as an arbitrary parameter with Q in the form of Equation (27). For the approximant with the index $[M/M, M]$ with P and R as in Equations (20) and (22), there will be $2M + 1$ remaining parameters, $p_0, \ldots, p_{\mathrm{M}-1}$ and $r_{-1}, r_0, \ldots, r_{\mathrm{M}-1}$, to be determined from the set of linear equations, Equations (5). The number of data points needed for this is

$$K = 2M + 1. \tag{29}$$

If the QA is applied only to the electronic energy, with P and R as in Equations (2) and (4), then the number of data points is

$$K = 2M. \tag{30}$$

With an odd number of data points the QA is to be applied to the total energy, and with an even number of points, to the electronic energy.

2.4. *Approximants constrained to empirical data*

As an alternative, instead of or in addition to parameterizing the approximant to *ab initio* energies, linear constraint equations can be formulated to incorporate empirical data such as the following:

(1) D_e, the ground-state well depth;

$$D_\mathrm{e} = E_{\mathrm{d},0} - E_\mathrm{e}, \tag{31}$$

where $E_\mathrm{e} = E(x_\mathrm{e})$. To impose this constraint, we can simply define the zero of energy as the bottom of the well, $E_\mathrm{e} = 0$, and then let $E_{\mathrm{d},0} = D_\mathrm{e}$. Evaluating the quadratic equation for E at x_e then gives the constraint

$$R(x_\mathrm{e}) = 0. \tag{32}$$

(2) x_e, the equilibrium bond distance;

$$\left.\frac{\mathrm{d}E}{\mathrm{d}x}\right|_{x_\mathrm{e}} = 0. \tag{33}$$

To impose this constraint, we take the derivative of the quadratic equation for E and then evaluate it at $x = x_\mathrm{e}$, with $E = 0$ and $E' = 0$. The result is

$$R'(x_\mathrm{e}) = 0. \tag{34}$$

(3) K_e, the harmonic force constant;

$$\left.\frac{\mathrm{d}^2E}{\mathrm{d}x^2}\right|_{x_\mathrm{e}} = K_\mathrm{e}. \tag{35}$$

Evaluating the second derivative of the quadratic equation at x_e, with $E'' = K_\mathrm{e}$, gives

$$R''(x_\mathrm{e}) - K_\mathrm{e}P(x_\mathrm{e}) = 0. \tag{36}$$

(4) The energy difference between the fragments from the two states,

$$\Delta_\mathrm{d} = E_{\mathrm{d},1} - E_{\mathrm{d},0}. \tag{37}$$

This sets the value of $E_{\mathrm{d},1}$.

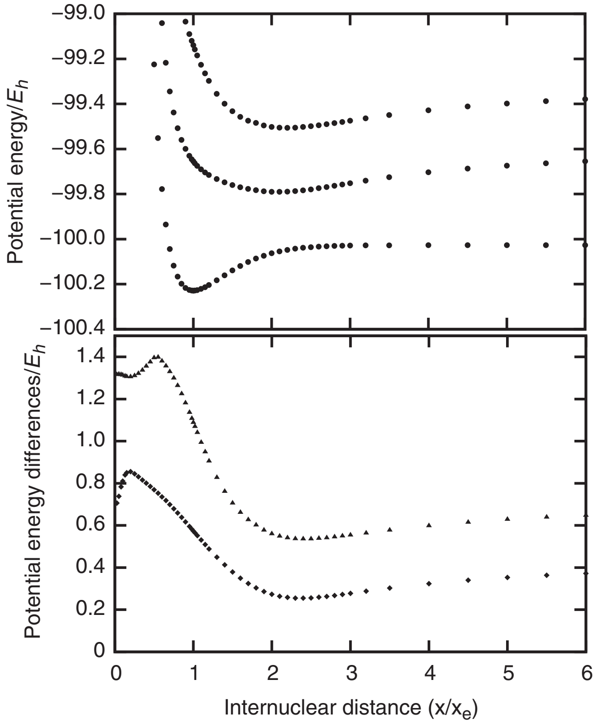

Figure 2. FCI potential energies for the electronic ground state of the hydrogen fluoride molecule and for the first two excited states of the same symmetry. The lower panel shows the energy difference between the ground state and the first excited state (diamonds) and between the ground state and the second excited state (triangles). Internuclear distance is given in units of the equilibrium bond length, $x_\mathrm{e} = 0.92025$ Å.

3. Applications

The accuracy of constrained quadratic approximants will now be examined using FCI energies for the hydrogen fluoride molecule. Two kinds of applications will be considered: (1) interpolation of *ab initio* energy values, and (2) the use of spectroscopic data to construct an empirical potential energy curve.

The FCI energies were computed with the cc-pVDZ basis set within the frozen core approximation using the PSI3 software package [22]. The values at dissociation were computed separately for the two fragments using the cc-pVDZ basis. The dissociation energy for the first excited state corresponds to a fluorine atom in its ground state and a hydrogen atom in a singly excited state.

The energy values for the ground state and for the first two excited states of the same symmetry as the ground state are plotted in Figure 2 and listed in Table 1. The lower panel of Figure 2 shows the energy differences between the ground state and the excited states. Note the points of closest approach, to the first

Table 1. FCI energies, in hartrees, for the hydrogen fluoride molecule as function of internuclear distance, in units of the equilibrium bond distance $x_e = 0.92025$ Å. The energies of the ground state and the first two excited states (of the same symmetry as the ground state) are shown. The basis set is cc-pVDZ.

x/x_e	Ground state	1st excited state	2nd excited state
0.025	79.985062	80.691363	81.300933
0.05	−20.926807	−20.188094	−19.609113
0.10	−68.296122	−67.485491	−66.982577
0.15	−82.689297	−81.838712	−81.382365
0.20	−89.416500	−88.561117	−88.111140
0.25	−93.206565	−92.361303	−91.896057
0.30	−95.545225	−94.714176	−94.223614
0.35	−97.059567	−96.243660	−95.722290
0.40	−98.068748	−97.268154	−96.712699
0.45	−98.753986	−97.968798	−97.377642
0.50	−99.225007	−98.455542	−97.829480
0.55	−99.551169	−98.798035	−98.152626
0.60	−99.777758	−99.041755	−98.397681
0.65	−99.935048	−99.217042	−98.578244
0.70	−100.043602	−99.344435	−98.713637
0.75	−100.117562	−99.438013	−98.818386
0.80	−100.166769	−99.507527	−98.902669
0.85	−100.198168	−99.559809	−98.973347
0.90	−100.216720	−99.599682	−99.034850
0.95	−100.226011	−99.630576	−99.089830
1.00	−100.228652	−99.654935	−99.139721
1.05	−100.226550	−99.674505	−99.185222
1.10	−100.221103	−99.690528	−99.226656
1.20	−100.204017	−99.715245	−99.297981
1.30	−100.182835	−99.733617	−99.354963
1.40	−100.160622	−99.748030	−99.399234
1.50	−100.139130	−99.759739	−99.432710
1.60	−100.119327	−99.769357	−99.457305
1.70	−100.101697	−99.777131	−99.474757
1.80	−100.086429	−99.783118	−99.484479
1.90	−100.073531	−99.787305	−99.495463
2.00	−100.062895	−99.789692	−99.502086
2.10	−100.054329	−99.790339	−99.505355
2.20	−100.047585	−99.789382	−99.506100
2.30	−100.042379	−99.787030	−99.504960
2.40	−100.038425	−99.783534	−99.502448
2.50	−100.035458	−99.779159	−99.498940
2.60	−100.033249	−99.774154	−99.494728
2.70	−100.031613	−99.768739	−99.490033
2.80	−100.030404	−99.763087	−99.485026
3.00	−100.028859	−99.751580	−99.474573
3.20	−100.028024	−99.740343	−99.464107
3.50	−100.027430	−99.724784	−99.449279
4.00	−100.027110	−99.703341	−99.428175
4.50	−100.027034	−99.686923	−99.411529
5.00	−100.027018	−99.674015	−99.398320
5.50	−100.027015	−99.663522	−99.387597
6.00	−100.027014	−99.654792	−99.378706
∞	−100.027013	−99.652555	

excited state at $x/x_e = 2.37$ and to the second excited state at 0.13 and 2.42. The ground-state energy function is expected in principle to have complex-conjugate branch point pairs with real parts approximately equal to these values.

3.1. *An* ab initio *potential energy curve*

Adding the constraints at $x \to 0$ and $x \to \infty$, we obtain the curves shown in Figure 3, interpolating between the nine circled points. These are from the [4/4, 4] approximant using $Q(x) = 1 + q_4 x^4$ as the denominator polynomial with $q_4 = 50$. The ground-state curve is insensitive to the choice of q_4, as long as it is positive. The singularity structure stabilizes for $q_4 > 40$, with two stable branch point pairs in the positive half-plane ranging only from $0.59 \pm 0.48i$ and $2.028 \pm 0.792i$ for $q_4 = 41$ to $0.58 \pm 0.33i$ and $2.020 \pm 0.779i$ in the limit of extremely large q_4, with all other singularities in the negative half-plane. With $q < 40$ there is an additional branch point pair, evidently spurious, that shifts with the value of q_4; its real part ranges from 0.0 for $q_4 = 40$ up to 1.95 for q_4 approaching zero.

There are true branch points in the positive half-plane at

$$2.05 \pm 0.77i, \quad 0.6 \pm 0.3i, \quad 0.2 \pm 0.3i.$$

These values were determined by noting the stable singularities in various approximants parameterized to points concentrated in the relevant regions of x. The singularity position at $x \approx 2$ is much more stable than those at $x < 1$. One can expect that there will be very many avoided crossings in the approach to the united atom limit as the molecular electronic spectrum degenerates to an atomic spectrum. The approximants have difficulty distinguishing between closely spaced branch points.

The most obvious benefit from imposing the constraints is that the branch of the approximant corresponding to the '+' sign in Equation (7) now gives a qualitatively reasonable description of the excited states. For $q_4 > 10$, this branch is insensitive to q_4. For smaller q_4 the upper branch of the QA becomes qualitatively incorrect, rising far above the FCI values. The figure shows the QA with $q_4 = 50$, but the curves from higher q_4 are virtually indistinguishable. Notice, though, that the '+' branch of the QA at large x describes the first excited state but at small x it switches to the second excited state. The QA has only two branches while the true $E(x)$ has many branches. The lower panel of Figure 2 showed an avoided crossing of the ground state with the first excited state at $2.37x_e$ and with the second excited state at $0.13x_e$.

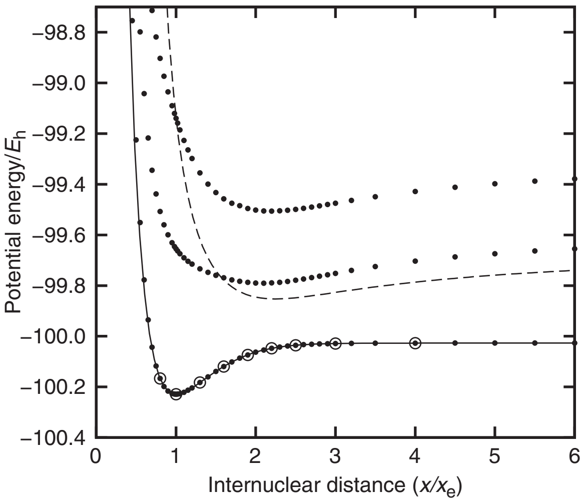

Figure 3. Potential energies for the ground state and the first excited state of the hydrogen fluoride molecule. The solid points are FCI energies. The solid and dashed curves show, respectively, the '−' and '+' branches of the [4/4,4] approximant with $q_4 = 50$, constrained by the nine circled points and by the $x \to 0$ and $x \to \infty$ limits.

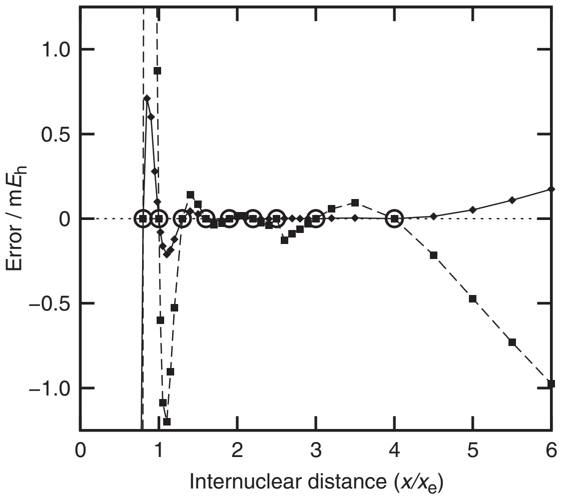

Figure 4. Error in the approximants for the ground-state energy with constraints and without constraints. Diamonds show the accuracy of the constrained [4/4,4] approximant of Figure 3 while squares show the unconstrained [1/3,3] approximant of Figure 1 (switching branches at $x/x_e =$ 2.2388).

The approximant's transition between the two excited states in Figure 3 occurs at the approximate midpoint of these two avoided crossings. The constraints improve the quantitative agreement for the ground state. This is shown in Figure 4, which compares the error with and without the constraints.

A possibly useful application of these approximants is to interpolate between regions of x that can be accurately treated with approximate quantum chemistry methods that are less costly than FCI. The accuracy of the commonly used approximate quantum chemical *ab initio* methods begins to fail as internuclear separations are stretched much beyond the equilibrium bond distances [23–26]. If the spin of the wavefunction is left unrestricted, then the accuracy improves at large separation, but in the intermediate region the accuracy typically remains rather poor. For hydrogen fluoride, the constrained QA can in practice interpolate through this intermediate region while staying well within 'chemical accuracy' of 1 kcal mol^{-1}, as demonstrated in Figure 5.

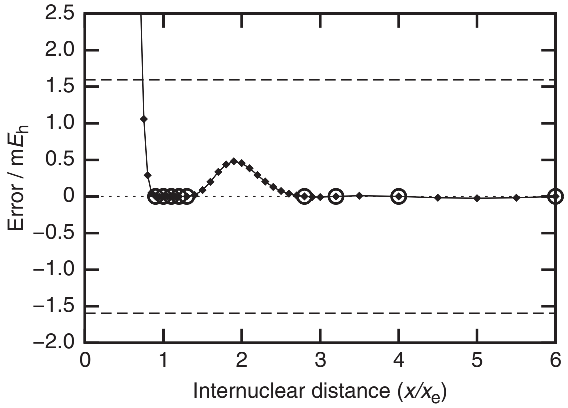

Figure 5. Error in the hydrogen fluoride potential energy curve from a constrained [4/4,4] QA interpolation, with $q_4 = 50$, parameterized at the nine data points indicated by open circles. Dashed lines show the limits for chemical accuracy, 1 kcal mol^{-1}.

The failure of approximate quantum chemistry computations in the intermediate region is due to the strong mixing between the zeroth-order reference wavefunction of the ground state with an excited state of the same symmetry [23]. In this case, for the QA of Figure 5, the mixing with the first excited state is described by a branch point pair in the QA at 1.969± 0.798i, with the real part in the centre of the region with no data points. It is interesting that the QA is able to give an accurate description of the mixing, accurately locating the branch point pair, even though it only uses data points in regions not obviously affected by it.

3.2. *An empirical potential energy curve*

Let us now consider the use of the constrained QA with the kind of data available from spectroscopic measurements, using simulated data derived from the FCI energies,

$$x_{\mathrm{e}} = 0.920250\,\text{Å}, \quad K_{\mathrm{e}} = 1.88047\,E_{\mathrm{h}}\,\text{Å}^{-2},$$
$$D_{\mathrm{e}} = 0.201639\,E_{\mathrm{h}}, \quad \Delta_d = 0.374459\,E_{\mathrm{h}}.$$

The QA is parameterized to these values as described in Section 2.4, with the additional constraint of the pole at $x=0$ with residue $\epsilon_{-1}=Z_{\mathrm{A}}Z_{\mathrm{B}}=9$. This is sufficient information to parameterize a [2/2,2] approximant with $Q(x)=1+q_2x^2$, where q_2 is arbitrary and with P and R as in Equations (20) and (22).

Figure 6 shows the locations of the branch points of the approximant as a function of q_2, with the value of q_2 ranging from 10^{-1} (the circled points) to 10^4, in logarithmic increments. For all q_2 values, the approximant has a branch point pair in the general vicinity of the true branch point at 2.05 ± 0.77i, but the singularity structure for $x < x_{\mathrm{e}}$ is less stable. For very large q_2 there is a single spurious branch point on the real axis between the true branch points 0.6 ± 0.3i. As q_2 drops to 20 this branch point shifts to midway between the true branch points at 0.2 ± 0.3i. Then it develops an imaginary part for smaller q_2.

This behaviour at $x < x_{\mathrm{e}}$ is typical of QAs [27,28]. If the parameterization is insufficient for the QA to simultaneously model multiple singularities, then it often happens that a single branch point is placed midway between the true singularities. This is a singularity in a region that is nonsingular. As a result, in the vicinity of this point the QA gives very poor accuracy.

No single value of q_2 for this system yields a qualitatively reasonable global potential curve. For approximants with the branch point on the real axis, the accuracy of the energy drops rapidly as the branch point is approached and then for smaller x the energy is a complex number. However, these approximants are qualitatively reasonable for $x > x_{\mathrm{e}}$. For $q_2 < 20$ the approximant gives a qualititatively accurate energy curve for small x but is highly *in*accurate for $x > x_{\mathrm{e}}$, giving a nonphysical second minimum. The best approach seems to be to use a small value for q_2 for describing the region $0 < x \leq x_{\mathrm{e}}$ and then a large value of q_2 for $x_{\mathrm{e}} \leq x$. Because the approximants are constrained to have the same value for $\tilde{E}$, $\tilde{E}'$, and $\tilde{E}''$ at x_{e}, these two functions are guaranteed to smoothly connect at x_{e}. This is demonstrated in Figure 7. Reasonable results left of x_{e} are obtained for any q_2 less than approximately 5 and right of x_{e} for any q_2 greater than approximately 50. The large-q_2 approximants also give a reasonable result for the excited state, for $x > x_{\mathrm{e}}$, but the small-q_2 approximants do not.

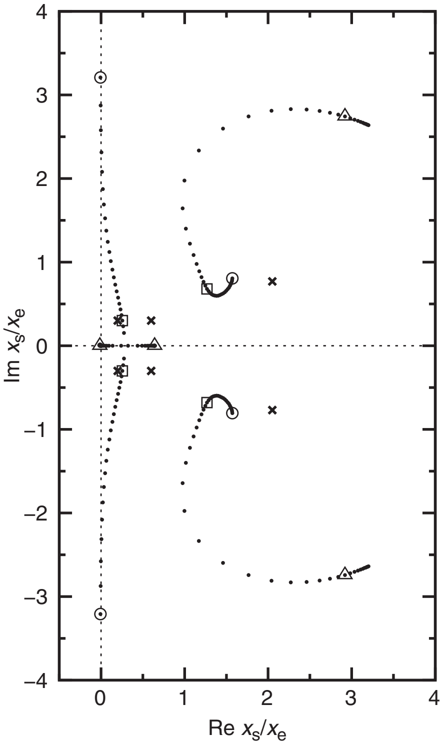

Figure 6. Locations x_s, in the complex plane, of branch points of the [2/2,2] quadratic approximant constrained according to Equations (31), (33), (35), and (37), as a function of the arbitrary parameter q_2. The solid points correspond to increments in $\log_{10} q_2$ by steps of 0.1 starting at $q_2=10^{-1}$ (the circled points), proceeding through 10^1 (the squares) and 10^3 (the triangles), ending at 10^4. The true positions of the branch points are marked with ×.

The dashed curve in Figure 7 shows the Morse potential [3],

$$E_{\mathrm{Morse}}(x) = D_{\mathrm{e}}\left(1 - \exp\left[(K_{\mathrm{e}}/2D_{\mathrm{e}})^{1/2}\,(x_{\mathrm{e}} - x)\right]\right)^2. \quad (38)$$

A clearer comparison of this with the QA is given by Figure 8, which shows the ground state energy in the vicinity of the equilibrium bond distance. The two curves have about the same overall level of accuracy but they work best in different regions. The Morse potential is significantly less accurate at $x < x_{\mathrm{e}}$ than the QA, due to the fact that it has a finite $x \to 0$ limit rather than the actual first-order pole. However, the Morse potential is more accurate than the QA for a moderately stretched bond. The accuracy of the QA for $x > x_{\mathrm{e}}$ can be systematically improved by adding additional constraint equations to incorporate anharmonicity corrections. It is also possible to modify the functional form of the Morse potential to give it the correct $x \to 0$ limit [5].

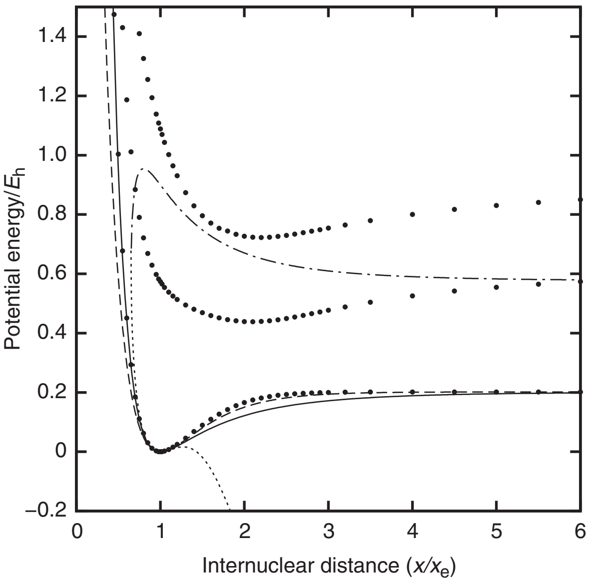

Figure 7. [2/2, 2] approximants constrained by the $x \to 0$ and $x \to \infty$ limits and by the values of x_e, D_e, K_e, and Δ_d. The QA with $q_2 = 1$ is shown as a solid curve for $x \le x_e$ and as a dotted curve for $x > x_e$ while the QA with $q_2 = 100$ is shown as a solid curve for $x \ge x_e$ and as a dotted curve for $x < x_e$. The dashed curve shows the Morse potential. The dash-dot curve shows the '+' branch of the QA with $q_2 = 100$.

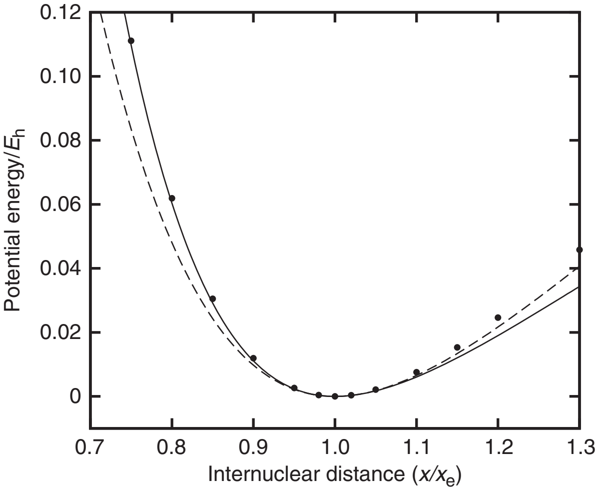

Figure 8. Comparison of the QA (solid curve, as in Figure 7) with the Morse potential (dashed curve).

4. Discussion

Quadratic approximants of a molecular potential energy curve, as formulated by Jordan [12,13], can accurately model the local analytic structure of the FCI electronic ground-state energy, with square-root branch points in the complex plane of the internuclear separation coordinate, x. It has been demonstrated here that with only minor modifications these approximants can yield a globally correct energy curve for the hydrogen fluoride molecule. An appropriate choice of approximant index ensures that both branches of the QA will approach finite constants in the limit $x \to \infty$. Constraining them to approach known values of the dissociated fragment energies improves the accuracy at intermediate x values. The usual formulation of the QA gives a finite $x \to 0$ limit. This neglects the first-order pole in the Coulomb potential between the two nuclei. Either the QA should be applied just to the electronic energy, with the internuclear potential added after the fact, or the form of the QA should be modified to include negative powers and constrained to have the known residue of the pole.

It is not surprising that explicitly building known limiting values into the approximants improves their accuracy. This has previously been shown to be the case for summation approximants for perturbation theories. In particular, the inspiration for this present study was the demonstration by Herschbach and coworkers [29–31] that the accuracy of low-order $1/D$ expansions, where D is the dimensionality of space, can be significantly improved at no added cost by incorporating a second-order pole at $D = 1$, so that the theory in effect becomes an interpolation between known limits at $D = 1$ and $D \to \infty$. Other techniques from perturbation theory, for example, the use of a conformal mapping to shift singularity positions to avoid spurious branch points in the approximant [28], might also be useful for interpolating potential energy curves.

A common problem with quadratic approximants is the occurrence of spurious singularities. For potential energy curves these come in three varieties:

(1) Pairs of nearly coincident branch points. This is the approximant's way of disposing of superfluous roots of the discriminant polynomial when there is not enough information for it to recognize true singularities. These are most damaging when they consist of a complex-conjugate pair with a very small imaginary part, in which case the 'excited state' of the approximant in effect drops below the 'ground state' with a very sharp avoided crossing. The accuracy is poor for the ground-state energy in the neighbourhood of the avoided crossing and the description of the excited state is qualitatively incorrect.

(2) An isolated branch point placed midway between two true branch points. The approximant senses singular behaviour but lacks the

resources to model both singular neighbourhoods. It 'compromises' with a single singularity in between. This is worse than if the approximant had not sensed any singularity structure, because a singularity is now being placed in a nonsingular region. If two true branch points are close to each other due to a small imaginary part, then the spurious branch point is placed on the real axis. On one side of this point the QA gives a complex number for the energy.

(3) Spurious poles at the roots of the denominator polynomial. These poles are present only in the excited-state branch and have only a small adverse effect on the accuracy for the ground state.

For the hydrogen fluoride molecule, spurious branch point pairs on the real axis can be eliminated by imposing the constraint that the two branches approach their respective dissociation energies for $x \to \infty$. This holds the two branches far enough apart in the important region of a just slightly stretched bond to prevent the spurious sharp avoided crossing. For a molecule that dissociates into identical fragments, the dissociation energies of the two branches can be expected to be the same and then this kind of spurious singularity might prove to be more of a concern.

The theory developed here introduces a free parameter, q_M, the coefficient of the denominator polynomial. The primary motivation for this was to avoid spurious poles in the excited state. However, this turned out to have the added benefit of mitigating the problem of an isolated spurious branch point on the real axis. It was found that q_M could be chosen so as to eliminate the branch point. It appears that a small value of q_M causes the QA to devote more of its resources to modelling the energy function at small x while a large value causes it to focus more on large x.

A drawback of quadratic approximants is the fact that they have only two branches, while the true FCI energy has many branches, one for each excited state. For this reason, the theory as developed here does not give a quantitatively correct description of the excited state. It describes avoided crossings involving the ground state but it does not describe avoided crossings between excited states. Jordan [13] has suggested replacing the quadratic equation, Equation (5), with a polynomial equation in $\tilde{E}$ of higher degree. A cubic equation, for example, would have three branches and this could include branch points connecting the second and third branches that would describe the effect of avoided crossings on the second branch. Algebraic approximants of arbitrary degree were proposed by Padé in his dissertation [20]. They have been studied by mathematicians [32] and have been used successfully to sum perturbation series for the Schrödinger equation [33,34], though they require a much larger data set for adequate parameterization than do quadratic approximants. Constraints could be imposed in a manner similar to that used here for the quadratic case, through additional linear equations. Higher-degree approximants would probably not significantly improve the description of the ground state but they might make it possible to use *ground*-state energy computations to quantitatively model the first excited state (of the same symmetry). Although the FCI method simultaneously yields results for excited states along with the ground-state energy, this is not true of most of the practical *ab initio* techniques, which typically just give results for the ground state. Direct methods for computing excited states are not nearly as well developed as methods for the ground state.

The theory and applications in the present study were developed for the FCI energy function, $\tilde{E}(x)$. It is interesting to consider whether or not the same conclusions hold for the true energy function $E(x)$. In the limit of infinite basis set dimension, the numerical value of $\tilde{E}(x)$ will approach that of $E(x)$. Because this holds true for any path around an isolated branch point of $\tilde{E}$, there must be a corresponding isolated branch point in E. However, it is possible for E to have other kinds of branch points than the square-root branch points that are the only kind in $\tilde{E}$. Many-body perturbation theories have critical points, corresponding to phase transitions, which correspond to a much more complicated kind of branch point that lies on the real axis [35,36]. $\tilde{E}$ models such a singularity with a grouping of square-root branch points in complex-conjugate pairs clustered closely about the critical point [19]. This is the kind of behaviour one can expect to see in a QA for a potential energy curve in which the ground state undergoes a sudden qualitative change in electronic structure as the molecular geometry is distorted.

References

[1] J.L. Dunham, Phys. Rev. **41**, 713, (1932); *ibid.* **41**, 721 (1932).

[2] M. Molski and J. Konarski, Int. J. Quantum Chem. **90**, 183 (2002).

[3] P.M. Morse, Phys. Rev. **34**, 57 (1929).

[4] D.W. Brenner, Phys. Rev. B **42**, 9458, (1990); *ibid.* **46**, 1948 (1992).

[5] R.J. Le Roy, C.C. Haugen, J. Tao and H. Li, Molec. Phys. **109**, 435, (2011) (doi: 10.1080/00268976.2010.527304) and references therein.

[6] D.W. Zhang, Y.M. Li and J.Z.H. Zhang, J. Theor. Comp. Chem. **2**, 119 (2003).

[7] X. Huang, B.J. Braams and J.M. Bowman, J. Chem. Phys. **122**, 044308, (2005) (doi:10.1063/1.2773714).

[8] Z. Xie, B.J. Braams and J.M. Bowman, J. Chem. Phys. **122**, 224307, (2005) (doi:10.1063/1.1927529).

[9] R.P.A. Bettens and M.A. Collins, J. Chem. Phys. **109**, 9728, (1998); and references therein.

[10] T. Ishida and G.C. Schatz, Chem. Phys. Lett. **324**, 369 (1999).

[11] T.-S. Ho and H. Rabitz, J. Chem. Phys. **119**, 6433, (2003) (doi:10.1063/1.1603219).

[12] K.D. Jordan, Chem. Phys. **9**, 199 (1975).

[13] K.D. Jordan, Int. J. Quantum Chem. Symp. **9**, 325 (1975).

[14] F. Jensen, *Introduction to Computational Chemistry* (Wiley, Chichester, England, 2001), Chap. 4.

[15] A. Katz, Nucl. Phys. **29**, 353 (1962).

[16] T.H. Schucan and H.A. Weidenmüller, Ann. Phys. **76**, 483 (1973).

[17] W.H. Miller, Adv. Chem. Phys. **25**, 69 (1974).

[18] M. Reed and B. Simon, *Methods of Mathematical Physics, IV: Analysis of Operators* (Academic Press, New York, 1978), Sec. XII.1, and references therein.

[19] A.V. Sergeev, D.Z. Goodson, S.E. Wheeler and W.D. Allen, J. Chem. Phys. **123**, 064105, (2005) (doi:10.1063.1.1991854).

[20] H. Padé, *Sur la Représentation Approchée d'une Fonction par des Fraction Rationnelles* (Gauthier-Villars, Paris, 1892).

[21] D.Z. Goodson, *Resummation Methods*, WIREs Comput. Mol. Sci. (2011) doi: 10.1002/wcms.92, and references therein.

[22] T.D. Crawford, C.D. Sherrill, E.F. Valeev, J.T. Fermann, R.A. King, M.L. Leininger, S.T. Brown, C.L. Janssen, E.T. Seidl, J.P. Kenny and W.D. Allen, J. Comput. Chem. **28**, 1610, (2007) (doi:10.1002/jcc.20573).

[23] G. Hose, J. Chem. Phys. **84**, 4505 (1986).

[24] D.Z. Goodson and M. Zheng, Chem. Phys. Lett. **365**, 396 (2002).

[25] A. Dutta and C.D. Sherrill, J. Chem. Phys. **118**, 1610, (2003) (doi:10.1063/1.1531658).

[26] S.E. Wheeler, W.D. Allen and H.F. Schaefer III, J. Chem. Phys. **128**, 074107, (2008) (doi:10.1063/1.2828523).

[27] D.Z. Goodson, J. Chem. Phys. **112**, 4901 (2000).

[28] D.Z. Goodson and A.V. Sergeev, Phys. Lett. A **359**, 481, (2006) (doi:10.1016/j.physleta.2006.06.071).

[29] D.R. Herschbach, J. Chem. Phys. **84**, 838 (1986).

[30] D.J. Doren and D.R. Herschbach, Chem. Phys. Lett. **118**, 115 (1985).

[31] D.Z. Goodson and D.R. Herschbach, Phys. Rev. A **46**, 5428 (1992).

[32] G.A. Baker Jr and P. Graves-Morris, *Padé Approximants* (Cambridge University Press, Cambridge, 1996), pp. 524–569, and references therein.

[33] A.V. Sergeev and D.Z. Goodson, J. Phys. A: Math. Gen. **31**, 4301 (1998), and references therein.

[34] F.M. Fernández, *Introduction to Perturbation Theory in Quantum Mechanics* (CRC Press, Boca Raton, Florida, 2001), pp. 126–136, and references therein.

[35] G.A. Baker Jr, Rev. Mod. Phys. **43**, 479 (1971).

[36] F.H. Stillinger, J. Chem. Phys. **112**, 9711, (2000) (doi:10.1063/1.481608).